Emergence of Charge-Transfer-to-Solvent Band in the Absorption Spectra of Hydrogen Halides on Ice Nanoparticles: Spectroscopic Evidence for Acidic Dissociation

Milan Ončák[†] and Petr Slavíček*,[†]

Department of Physical Chemistry, Institute of Chemical Technology Prague, Technická 5, Prague 6, Czech Republic

Viktoriya Poterya and Michal Fárník[‡]

J. Heyrovský Institute of Physical Chemistry, v.v.i., Academy of Sciences of the Czech Republic, Dolejškova 3, 182 23 Prague 8, Czech Republic

Udo Buck

Max-Planck Institut für Dynamik und Selbstorganization, Bunsenstrasse 10, D-37073 Göttingen, Germany

Received: February 11, 2008; Revised Manuscript Received: March 31, 2008

Extensive *ab initio* calculations complemented by a photodissociation experiment at 193 nm elucidate the nature of hydrogen halide molecules bound on free ice nanoparticles. Electronic absorption spectra of small water clusters (up to 5 water molecules) and water clusters doped with hydrogen fluoride, hydrogen chloride and hydrogen bromide were calculated. The spectra were modeled at the time-dependent density functional (TDDFT) level of theory with the BHandHLYP functional using the reflection principle. We observe the emergence of a charge-transfer-to-solvent (CTTS) band in the absorption spectra upon the acidic dissociation of the hydrogen halides. The CTTS band provides a spectroscopically observable feature for the acidic dissociation. The calculated spectra were compared with our new experimental photodissociation data for larger water clusters doped with HCl and HBr. We conclude that HCl and HBr dissociate to a large extent on the surface of ice nanoparticles at temperatures near 120 K and photoactive products are formed. The acidic dissociation of HX leads to an enhancement by about 4 orders of magnitude of the HCl photolysis rate in the 200−300 nm region, which is potentially relevant for the halogen budget in the atmosphere.

I. Introduction

Hydrogen halides (HX), in particular HCl, are important species in atmospheric chemistry.[1,2] The atmospheric relevance of these molecules is closely related to their photochemistry. Hydrogen halides after a photoexcitation into the first electronic absorption band dissociate into hydrogen and halogen atoms, forming thus reactive forms of halogens. Halogen radicals are especially important in the stratosphere where these atoms serve as efficient catalysts of the ozone decomposition reaction. The maximum of the first absorption band is located at 120 nm for HF, 154 nm for HCl and 178 nm for HBr. The electronic absorption of bare HX starts below 155 nm for HF, 200 nm for HCl and 250 nm for HBr. Neither of these molecules absorbs above 290 nm and the photolysis of HX is thus not an important reaction in tropospheric chemistry. It is also considered that, even in the stratosphere, the photolysis rate is slow enough so that HX can act as a temporary halogen reservoir.

Hydrogen halides adsorb on the surface of polar stratospheric clouds (PSC). On these particles, various heterogeneous reactions can convert hydrogen halides (HCl in particular) into halogen molecules (Cl_2) absorbing at higher wavelengths. Molecular chlorine is then easily photolyzed during the polar spring. These reactions are referred to as "chlorine activation reactions".[3]

The discovery of HCl being the most abundant chlorine reservoir during processes on PSCs initiated numerous experimental and theoretical studies devoted to the exploration of the hydrogen chloride−ice system. In particular, the uptake process of HCl on ice and chlorine activation reactions have been extensively studied.[4,5]

The fate of HCl upon the uptake on ice particles remains controversial despite a great effort devoted to this issue. The behavior of hydrogen halides differs with the type of ice, temperature and surface coverage. HCl and HBr and under certain conditions also HF can react with water molecules to form X^- and H_3O^+ or $H_5O_2^+$ ions.[6–11] The general conclusion emerges as follows. At very low temperatures, HCl stays intact on the ice surface, whereas with increasing temperature, it starts to dissociate. For isolated hydrogen halides on ice surfaces, the transition between an intact and dissociated form probably takes place between 80 and 120 K. The process of HX dissociation on ice was studied using infrared spectroscopy,[6–8] reactive ion scattering,[12,13] X-ray absorption spectroscopy,[14] various other surface analysis methods,[15] and most recently H-photofragment time-of flight spectrometry.[16] The structure of the ice surface doped with HCl or HBr has also been addressed theoretically.[6,7,17]

The HX−water system has also been investigated in a cluster state.[8,18–27] Clusters are convenient for comparison of theoretical calculations and experimental results. However, it is important

* Corresponding author. E-mail: petr.slavicek@vscht.cz.
[†] Also at J. Heyrovský Institute of Physical Chemistry, v.v.i., Academy of Sciences of the Czech Republic, Dolejškova 3, 182 23 Prague 8, Czech Republic.
[‡] E-mail: michal.farnik@jh-inst.cas.cz.

10.1021/jp8012305 CCC: $40.75
Published on Web 05/29/2008

to emphasize that especially small water clusters have a different structure than that found for ice. This is because water molecules in ice are chemically bound in a lattice structure. In clusters, on the other hand, they can more freely adjust their position. The onset of HCl and HBr acidic dissociation is found for HX interacting with four water molecules. Even for the HF the acidic dissociation has been predicted for some cluster sizes at zero temperature.[23] The structural arrangement as that found in small water clusters is not easily reached on the warm ice surface and for large molecular clusters. In a combined experimental and computational study it was found that pure water clusters larger than $N = 300$ have a crystalline core and a disordered surface layer with a decrease of 3-coordinated molecules.[28] Thus strong adsorbates like HCl and HBr acids are stabilized at low temperatures but start to bind and dissociate at higher temperatures. We note that ice[4] and also solid neon clusters[29] form a quasi-liquid layer on the surface.

The photochemistry and photophysics of the HCl−ice system has not been exploited to the extent to which its physics and chemistry in the ground state has been studied; *i.e.*, much less is known about the excited states of these systems. The obvious reason is that hydrogen halides are considered to be photochemically relatively intact reservoir species. Toubin *et al.*[30,31] have performed quantum dynamical simulation of HCl on ice surfaces. Their results support the idea of HCl as a photochemically stable molecule in the atmosphere. Also, the photodynamics of the HBr− and HI−water clusters was investigated experimentally.[32,33] Sobolewski and Domcke[34–36] have studied small HCl−water clusters in the context of a solvated electron. They found that upon the electronic excitation of a solvent separated pair $H_3O^+(H_2O)_3Cl^-$, a neutral biradical $H_3O(H_2O)_3Cl$ is energetically accessible. This electronic transition is of a charge-transfer-to-solvent (CTTS) character and leads, in this particular case, to a lowering of the S_1/S_0 gap.

We have recently found that exploring the photochemistry of the HX−water nanoparticles can shed light on a ground state structure of these particles.[37] We have studied the photodissociation at 193 nm of $HX-(H_2O)_N$, $DX-(H_2O)_N$ and $HX-(D_2O)_N$ ($X = Br, Cl$; $N \approx 500$) experimentally. The estimated temperature of these clusters corresponds to 100−130 K. There have been two major findings: (i) only slow hydrogen atoms have been produced; (ii) hydrogen atoms H have been generated for all three isotope combinations, with a signal ratio of approximately 3:2:1, respectively. Note that the dissociated hydrogen production from bare water clusters has been found to be negligible at these conditions. The double isotope experiment suggests an isotope mixing between HX and water. We have postulated the H_3O radical (and its isotopic variants DH_2O and D_2HO) to be the key species in the HX−water photochemistry, explaining both the isotope mixing and hydrogen kinetic energy distribution. The metastable H_3O radical can be formed in two ways.

Mechanism A: Acidic Dissociation Followed by an Electronic Excitation

$$HX \cdot (H_2O)_N \rightarrow X^- \cdot H_3O^+ \cdot (H_2O)_{N-1}$$

$$X^- \cdot H_3O^+ \cdot (H_2O)_{N-1} + h\nu \rightarrow X \cdot H_3O \cdot (H_2O)_{N-1}$$

Mechanism B: Direct Electronic Excitation of HX

$$HX \cdot (H_2O)_N + h\nu \rightarrow X \cdot H_3O \cdot (H_2O)_{N-1}$$

The final step in both cases is the hydronium dissociation:

$$X \cdot H_3O \cdot (H_2O)_{N-1} \rightarrow H + X + (H_2O)_N$$

We have concluded that the acidic dissociation mechanism A is more consistent with the experimental observations. In this work we further support this conclusion by a quantitative comparison of the relative H-atom photodissociation yield from $HCl(H_2O)_n$ and $HBr(H_2O)_n$ system with the electronic absorption spectra calculated at the *ab initio* level for the HX−water clusters. We further argue that the photochemistry of hydrogen halides is potentially more relevant for the atmospheric chlorine radical balance than could be anticipated from the gas phase data. We exploit the advantage of theory that various processes can be investigated even if they do not take place in the experiment. Here, we calculate electronic absorption spectra for small water clusters at different states: with intact HX, contact ion pair and solvent separated ion pair structures. These three structural motifs can also be potentially found in larger clusters. Note that we have calculated the shapes of the electronic absorption spectra, *i.e.*, not only the positions of the peaks but also their widths. Recently, also the electronic spectroscopy of water clusters and bulk water[38–44] as well as the photodissociation dynamics of ice[45–48] have attracted considerable attention. We have also calculated the electronic absorption spectra for bare water clusters for comparison.

It is impossible to measure the direct absorption for clusters in our experiment. We have deduced the relative absorption cross section from the measurement of the hydrogen atom yield produced by the photodissociation of HCl and HBr molecules in the gas phase, HCl and HBr molecules deposited on the surface of argon clusters, HCl and HBr molecules attached to large water clusters, and also for bare water clusters. The measurements for bare hydrogen halides are important for the validation of our method as a tool for determining the relative absorption cross sections, because the absolute cross sections for these systems are available in this case. Argon clusters represent a structureless inert solvent. Hydrogen halides can not react with argon atoms but the hydrogen fragment can be slowed down by the *cage effect*.[49,50] Only in the case of water can HX also react with the solvent particles.

II. Methods

A. Electronic Structure Calculations. Ground state geometries and energetics have been calculated using the Møller−Plesset perturbation theory (MP2) and density function theory (DFT) with the BHandHLYP functional. For hydrogen and all heavy atoms except bromine, the 6-31++g** basis has been used. For bromine, we have employed the Stuttgart RLC effective core potential (ECP28MWB)[51] with the corresponding basis set augmented with additional s and p diffusion functions (with exponents of 0.074 and 0.018) and d function with an exponent of 0.601.

In this paper, we aim to quantitatively compare relative absorption cross sections with the experiment. The choice of the method for the electronic structure calculations of the electronic electronic excitation energies is therefore of major importance. The time-dependent density functional theory (TDDFT) approach is computationally relatively inexpensive. However, the functional must be selected with a maximal care. TDDFT methods are often not able to treat adequately charge-transfer (CT) states, producing spurious CT states. This might be problematic especially for large systems.[52] This problem is not present in the equation of motion of the coupled clusters (EOM-CCSD) method which is, however, a much more demanding approach. Because both of the above approaches rely on a single reference wave function, we have compared

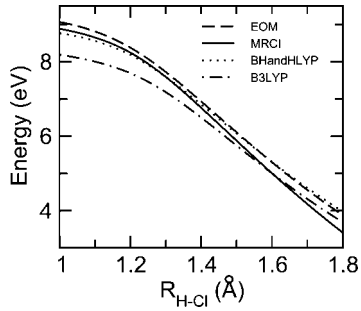

Figure 1. Difference between the ground and first excited state of HCl calculated at the several levels of theory.

TABLE 1: Experimental Conditions

cluster gas	H_2O	Ar
nozzle diameter (μ m)	75	60
conical nozzle opening angle (deg)	30	30
expansion pressure p_0 (bar)	5.3	4.1
nozzle temperature T_0 (°C)	175	−40
mean cluster size $\bar{n}$	400	100

our results with the multireference configuration interaction method including single and double excitations (MRCI).

During the evaluation of each electronic absorption spectrum, 1000 excitation energies were collected, so the TDDFT method was the only practical way to perform this task. We have used the BHandHLYP functional because (i) this functional reasonably well describes hydrogen-bonded systems[53] and (ii) spurious charge-transfer states are less likely to occur due to the inclusion of a large portion of the Hartree−Fock exchange.[52] It is nevertheless needed to validate this choice against other methods. Figure 1 shows the difference between the ground and first excited state of HCl molecule at the DFT/BHandHLYP, DFT/B3LYP, EOM-CCSD and MRCI levels. The B3LYP functional provides electronic excitation energies that are lower than the experimental value obtained from the maximum of the first absorption band (7.28 eV at B3LYP level *vs* 8.1 eV). The BHandHLYP functional on the other hand gives results similar to the EOM-CCSD results in the whole range of bond lengths. At larger HCl separations, both the EOM-CCSD and the TDDFT/BHandHLYP electronic excitation energies deviate from the corresponding MRCI calculation. This deviation is caused by an increasingly multireference character of the HCl molecule upon stretching. These distances, however, are not relevant for an electronic absorption spectrum description. We have tested the performance of the DFT/BHandHLYP method (both electronic excitation energies and transition dipole moments) for representative clusters up to $HX(H_2O)_4$ and also for these systems a good agreement between TDDFT and a more demanding wave function based methods has been found. We conclude that the TDDFT/BHandHLYP approach describes decently the excitation process of $HX(H_2O)_N$ clusters, in both the intact and acidically dissociated state.

The Molpro06[54] program package has been used for the MRCI and EOM-CCSD calculations. The MP2, DFT and TDDFT calculations have been performed using the Gaussian03[55] package.

B. Electronic Absorption Spectra Calculations. Calculation of the absorption spectrum for multidimensional systems is generally a demanding task. Here, we have utilized the multidimensional reflection principle.[56] The method is based on the assumption that the absorption spectrum reflects a ground state vibrational wave function (multiplied by the respective transition probability). Reflection methods work well for dissociative processes, all recurrences of a wave function (and therefore resonances in spectra) are neglected. It has been shown that even for simple cases as the HCl photodissociation, the calculated spectrum is not completely identical with the spectrum obtained by a full quantum dynamical calculation.[57] On the other hand, the reflection principle is a simple approach that can be used for the *ab initio* calculation of the electronic absorption spectra.

In the reflection principle approach a ground state wave function φ_0 is projected onto an excited state curve and further onto an energy axis; the width of the spectrum is related to the width of the ground state wave function and the slope of the excited state curve. The absorption cross section $\sigma(\omega)$ for the excitation frequency ω is given by

$$\sigma(\omega) = \frac{\pi\omega}{3c\hbar\varepsilon_0}\langle\varphi_0|\mu_{0k}^{*}\delta(E_0/\hbar + \omega - \hat{H}_k/\hbar)\mu_{0k}|\varphi_0\rangle \quad (1)$$

$$= \frac{\pi\omega}{3c\hbar\varepsilon_0}\int \mathrm{d}\vec{\tau}|\varphi_0|^2|\mu_{0k}|^2\delta(E_0/\hbar + \omega - \frac{1}{2}E_{ZPE}/\hbar - \hat{V}_k/\hbar) \quad (2)$$

where μ_{0k} stands for the transition dipole moment for the excitation from the ground state 0 with energy E_0 to the excited state k with the time-independent Hamiltonian $\hat{H}_k$. The kinetic energy of the excited state may be approximated by one-half of the zero-point energy of the ground state E_{ZPE}, therefore $\hat{H}_k = {}^1/_2E_{ZPE} + \hat{V}_k$. We have employed Monte Carlo techniques to evaluate the multidimensional integral in the above equation.

To calculate absorption spectra by using the reflection principle, we need to sample a ground state wave function or, at finite temperature, the corresponding density matrix. This can be easily done within the harmonic approximation. Beyond the harmonic approximation, one could sample the initial wave function using path integral techniques.[58] However, *ab initio* quantum simulations are still computationally rather prohibitive. For the low frequency anharmonic modes, the quantum distribution converges rapidly with temperature to the classical one generated, *e.g.*, by classical molecular dynamics. The shape of absorption spectra is, however, given mostly by high frequency (harmonic) modes. We have therefore adopted a different approach. Internal modes can be divided into two sets: either we deal with essentially harmonic modes which are highly quantum or we deal with anharmonic modes. Contribution of the latter set to the shape of electronic absorption spectra is neglected. For our systems, we have chosen the threshold of 500 cm^{-1}. The spectrum is at this point essentially converged (with respect to adding further modes) whereas the modes are still reasonably harmonic. Note that an absorption spectrum calculated with the classical ground state distribution at different temperatures is very narrow which suggests that the shape of a spectrum is dominated by the high-frequency harmonic modes.

For each species (*i.e.*, for each cluster), 1000 points were sampled from the initial harmonic wave function. At each geometry, all electronic excitation energies above a certain threshold (140 nm for intact and 150 nm for contact and separated ion pair structures) were collected. Harmonic wave functions were calculated at the MP2/6-31++g** level.

C. Photodissociation Experiments in Molecular Clusters. The above calculated cross sections can be compared with the experimental results of the photolysis of hydrogen halide molecules on water clusters. Experimental methods have been described in more detail elsewhere.[59] Briefly, the water cluster beam was produced by a supersonic expansion of neat water vapor through a conical nozzle. The nozzle parameters and the expansion conditions, summarized in Table 1, determined the mean cluster size $\bar{n} \approx 400$.[60] The internal temperature of

the clusters has been estimated using the condensation model outlined in ref 61 to be 100−130 K. After passing through a skimmer and a following differentially pumped vacuum chamber, the cluster beam entered a pick up cell filled with the molecular HX gas. The pick-up gas pressure was kept low to ensure a single HX molecule pick-up in the majority of cases.

Clusters with attached molecules then entered a vacuum chamber with two-stage time-of-flight spectrometer of Wiley−McLaren type (WMTOF), where the molecules were photolyzed with 193 nm laser light. H-fragments were successively ionized by the (2 + 1) REMPI process with 243.07 nm laser. The WMTOF spectrometer was used to measure the time-of-flight (TOF) spectra of H atoms arising from the photodissociation process. To obtain the fragment velocity distributions, the WMTOF was operated in a low-field mode with a small electric field of 4.7 V/cm applied to extract the ions to the detector.

The 193 nm radiation was produced by an ArF/F_2 excimer laser (Lambda: Compex 102). The wavelength of 243.07 nm was generated by mixing the fundamental of a Nd:YAG laser (Quanta Ray GCR-5) with the frequency doubled output of a dye laser (LAS, LDL 20505) operated at 630.3 nm, and pumped by the second harmonic of the Nd:YAG laser.

For comparison, experiments were performed with the photolysis of HX molecules on rare gas Ar_n, $\bar{n} \approx 100$, clusters (Table 1). In addition, a comparison with the photodissociation of the gas phase HX molecules was made. In this case, using a molecular beam of HX resulted in contamination with $(HX)_N$ cluster photolysis. Therefore, we have used a different approach, where the cluster beam was blocked and the HX pressure in the pick-up cell was increased to yield a measurable signal from the dissociated HX molecules, which diffused from the pick-up cell into the laser interaction region in the WMTOF chamber. It should be mentioned that background originating from diffused HX molecules was carefully subtracted in the cluster beam experiments.

Finally, it ought to be mentioned that the direct quantitative comparison of H-fragment signals between HBr and HCl systems was only possible in exceptional cases, as discussed in the Results. The measured H-fragment signal was, indeed, proportional to the total photodissociation yield, which in turn was proportional to the absorption cross section. However, because the TOF spectra were measured with a low electric field applied in the extraction region of the WMTOF spectrometer, the detection probability for an H-fragment depended strongly on the initial H-fragment velocity after the photolysis. Therefore, generally, the signals should be compared after the TOF conversion to the kinetic energy distribution (KED), which includes the energy dependent detection probability. In the conversion procedure the experimental points were fitted with a Monte-Carlo (MC) simulation of the particle trajectories in the photodissociation process, which was carried out considering the molecular beam data, the photodissociation process parameters, the WMTOF geometry, the finite interaction volume, and the detector electronic response.[62]

III. Results

A. Ground State Cluster Structure. As has been discussed in the Introduction, there are three major structural motifs for HX on water clusters. The first structural type consists of hydrogen halide remaining in a covalent state ($HX(H_2O)_N$), this state will further be referred to as "intact". Upon the acidic dissociation, the oxonium cation and halogenide anion can remain in the closest proximity (contact ion pair, $X^-H_3O^+(H_2O)_{N-1}$) or these ions can be separated by water solvent molecules (solvent separated structure, $X^-(H_2O)_{N-1}H_3O^+$).

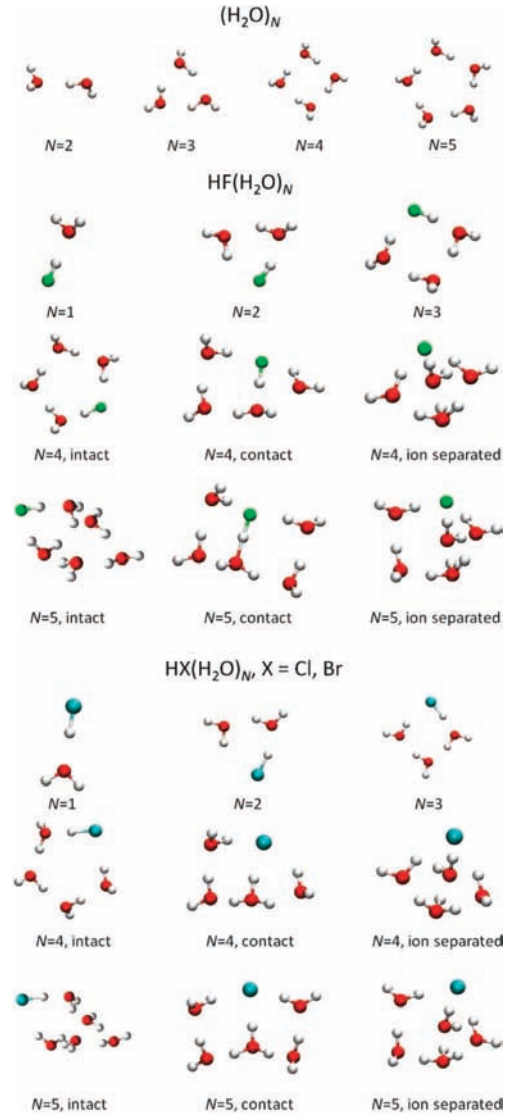

Figure 2. Calculated structures of the clusters studied. For relative energies, see Table 2.

Figure 2 shows optimized structure of $(H_2O)_N$, $HF(H_2O)_N$, $HCl(H_2O)_N$, and $HBr(H_2O)_N$ clusters ($N = 1-5$) for which the electronic absorption spectra have been calculated. Respective energies are given in Table 2. The structural effect of quantum delocalization can be for weakly bound systems quite important.[63,64] Also, thermal effects influence structures of these systems.[27] Zero point effects change the relative energy ordering of different isomers for certain $HX(H_2O)_N$ clusters. However, we use the structures in Figure 2 only as examples of the three structural motifs and the exact ordering of structures is not a prime interest of this paper.

For clusters with $N = 1-3$, the only local minima found are the intact structures. For clusters with $N = 4, 5$, there are present all three types of structural motifs: intact structure, solvent separated and contact ions. From the relative energies at several levels of theory, it is found that HCl and HBr clusters are predicted to support dissociated states starting from $N = 4$. The general picture of the HX dissociation process is in agreement with previously reported calculations.[18,20,24]

Hydrogen fluoride is a weak acid in the bulk. However, solvent separated pair represents a local minimum for clusters starting from 4 water molecules attached to HF. We were not able to find a truly contact ion structure. Closest to the contact

TABLE 2: Relative Energies (kcal/mol) of the $HX(H_2O)_N$ Isomers (X = F, Cl, Br; N = 4, 5) at the MP2 and DFT/BHandHLYP Level of Theory[a]

	DFT			MP2		
molecule	intact	contact	separated ion	intact	contact	separated ion
$HF(H_2O)_4$	0.00 (0.00)	4.23 (3.81)	12.51 (13.15)	0.00 (0.00)	3.81 (3.27)	11.60 (11.97)
$HF(H_2O)_5$	0.16 (1.69)	0.00 (0.00)	6.18 (7.15)	0.00 (0.70)	0.40 (0.00)	6.02 (6.45)
$HCl(H_2O)_4$	2.76 (0.00)	2.57 (2.04)	0.00 (0.33)	0.00 (0.00)	2.21 (3.75)	0.52 (3.30)
$HCl(H_2O)_5$	5.09 (3.68)	0.16 (0.00)	0.00 (0.02)	1.35 (0.00)	0.00 (0.09)	0.35 (0.69)
$HBr(H_2O)_4$	6.73 (3.31)	2.03 (1.69)	0.00 (0.00)	2.90 (0.00)	1.92 (1.59)	0.00 (0.35)
$HBr(H_2O)_5$	8.99 (7.15)	0.75 (0.61)	0.00 (0.00)	4.27 (2.11)	0.29 (0.15)	0.00 (0.00)

[a] Zero-point corrected energies are added in parentheses. For HF, contact ions have a structure of a Zundel type. Energies are related to the global minima of respective clusters. For isomer structures see Figure 2. Basis set used is described in the Methods.

ion structure motif was a structure with highly elongated H−F bond distance. Hydrogen can be for these structures quite delocalized and the resulting species can be described as a Zundel type structure. Note that the Zundel type structures have been recently spectroscopically identified for the HF adsorbed on ice (T = 40 K).[11] It should be also mentioned that a global minimum structure with dissociated HF on a water cluster has recently been localized for N = 7.[23]

B. Electronic Structure of $HX(H_2O)_N$ Clusters. The first excited state of isolated water can be interpreted in terms of a single excitation from an oxygen 2p orbital into a partially antibonding orbital of the OH bond and a partially Rydberg orbital. In water clusters, the oxygen atom of an excited water molecule is positively charged and its interaction with a neighboring positively charged ground state hydrogen leads to the overall blue shift of the first absorption band. The water dimer is an exception for one oxygen is not connected to any hydrogen *via* a hydrogen bond. This results in a red tail in the electronic absorption spectrum: the excited state is even stabilized by a neighboring ground state water molecule.[38] Note that for large clusters the electronic excitations are delocalized. Upon the electronic excitation to the first absorption band, water dissociates.

The character of the electronic excitation into the first excited state for hydrogen halides is very similar to that for a water molecule. An electron is excited from a nonbonding orbital of a halogen atom X to an antibonding orbital of the X−H bond with a strong Rydberg mixing. As a result, the H−X bond dissociates. The first absorption band of hydrogen fluoride is lying at much shorter wavelengths than for an isolated water molecule. Therefore, the low lying excited states of HF−water clusters can be attributed to the excitations within the water part of the system. Hydrogen fluoride acts as a ground state spectator. This remains true even after the acidic dissociation of HF.

The excited state of the small water clusters doped with a hydrogen chloride have been studied in detail by Sobolewski *et al.*[34] in the context of a solvated electron. The HOMO of a water molecule is energetically located slightly below the hydrogen chloride HOMO and by about 1.0 eV below the hydrogen bromide HOMO and the positions of the LUMOs are rather close. For mixed clusters $HX(H_2O)_N$, the first excited state can therefore include also excitations from HX orbitals to antibonding or Rydberg orbitals of water. The character of the excitation in the first absorption band for $HX(H_2O)_N$ can be described as a single excitation from a nonbonding orbital of a halogen atom to a molecular orbital which is a mix of a H−X antibonding, HX Rydberg, water Rydberg and water antibonding orbital. Our excited state dynamical calculations suggest that the excitation is mostly localized on HCl leading to its dissociation. On the other hand, HBr can "catalyze" water dissociation. This is in accord with the position of the HOMO orbitals for water, HBr and HCl. We thus observe limited charge transfer even from HX to water molecules.

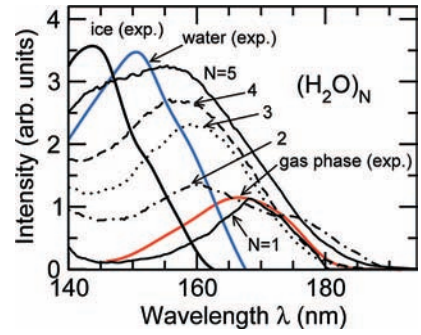

Figure 3. Calculated absorption cross section for $(H_2O)_N$ clusters of various sizes N = 1...5. The geometries of the respective clusters are shown in Figure 2. For comparison also the experimental results for the gas phase molecule,[66] liquid water[67] and ice[68] are presented.

After the acidic dissociation, the HOMO orbital of the halogen anion is shifted further up (1.4 eV for $HCl(H_2O)_4$) and the charge-transfer-to-solvent (CTTS) state is shifted to much lower energies. The electronic excitation can be described as a transfer of an electron from a p orbital of the anion to the H_3O moiety. Our dynamical calculations show that after the photoexcitation, the halogen atom starts to dissociate from the water cluster. However, Sobolewski *et al.* have found a stable biradical structure after the umbrella inversion of the H_3O radical together with water molecules to which it is bound. This structure indeed represents the minimum on the S_1 potential energy surface. This state is energetically accessible; however, the chlorine dissociation will occur on a fs time scale and the biradical minimum is not reached during the photodissociation process. Water−water transitions for the HCl and HBr clusters appear above 8 eV.

C. Electronic Absorption Spectrum of Pure Water Clusters. Figure 3 summarizes calculated electronic spectra of water clusters $(H_2O)_N$, N = 1−5 . Absorption maxima shift to larger energies with an increasing size of the clusters. As explained above, this can be rationalized due to a Coulombic repulsion between a positive charge of the excited water oxygen and a positive charge of a corresponding ground state water hydrogen.[38] The increasing width of the first absorption band is related to a vibrational delocalization (hydrogen bonding leads to a lowering of the O−H bond vibrational frequency) and also to the fact that more states are involved, *i.e.*, not only states localized on a single water molecule but also an excitation from the HOMO orbital of one water molecule to orbitals localized at different molecules. Furthermore, spectra of N = 2−5 water clusters show the absorption in the 180−205 nm region, this "red tail" was predicted for a water dimer[38] and also confirmed experimentally.[65]

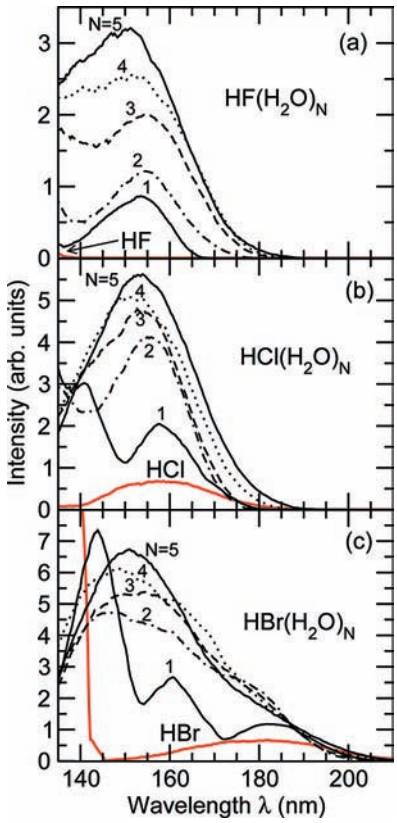

Figure 4. Calculated absorption cross section for intact structures of (a) $HF(H_2O)_N$, (b) $HCl(H_2O)_N$, and (c) $HBr(H_2O)_N$ clusters of various sizes $N = 1, \ldots, 5$. The geometries of the respective clusters are shown in Figure 2.

Water clusters have two limits for which the absorption cross section can be measured: an isolated molecule and bulk. In Figure 3 experimental absorption spectra for an isolated water molecule,[66] liquid water[67] and ice[68] are added. There is a satisfactory agreement between our calculated monomer absorption spectrum and the measured one. Minor discrepancies can be assigned mostly to the electronic structure method used. The absorption spectrum then evolves in the direction of ice and liquid water. It is clear that the ice (bulk water) limit is not fully reached within five molecules. We can, however, see the rise of certain characteristic features. In particular, already for 5 molecules we can trace the onset of the 140 nm peak; the maximum has shifted from 170 nm in the gas phase to 150 nm for $(H_2O)_5$.

D. Size Evolution of $HX(H_2O)_N$ Electronic Absorption Spectra. Electronic absorption spectra for intact $HX(H_2O)_N$ clusters are shown in Figure 4. The computed absorption maximum for the bare molecules in the first absorption band is 182 nm for HBr, 168 nm for H_2O, 157 nm for HCl, 123 nm for HF.

Bare hydrogen fluoride starts to dissociate at about 140 nm. Complexed with water molecules, the absorption in the first absorption band in UV region is given mostly by the absorption of water molecules rather than by HF. Hydrogen fluoride has, however, a profound effect on the water absorption spectrum. For the $HF-H_2O$ complex, the spectrum is shifted to the blue by 0.7 eV. This is caused by the same electrostatic effect which shifts the absorption spectrum of a water dimer, only now the donor molecule (HF) absorbs at much lower wavelengths. With increasing number of water molecules, the spectrum converges to the one of water clusters.

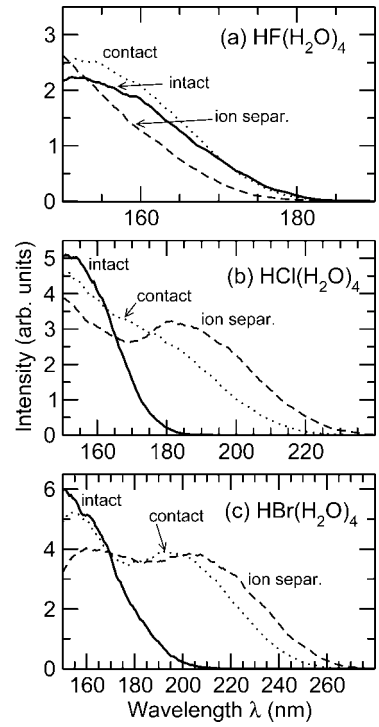

Figure 5. Calculated absorption cross sections for the intact, contact and solvent separated structures for (a) $HF(H_2O)_4$, (b) $HCl(H_2O)_4$, and (c) $HBr(H_2O)_4$ systems. The geometries of the respective clusters are shown in Figure 2.

The electronic absorption spectrum of both HCl and HBr is much broader than the absorption spectrum of bare water molecule. The experimental absorption spectra for bare HCl and HBr are reasonably well reproduced in our calculations. The difference at high energies is mostly connected to the electronic structure method rather than to the use of the reflection principle. The maximum of the first absorption band for HCl (157 nm) is blue-shifted with respect to the water absorption maximum. However, at 193 nm HCl already absorbs 50 times more than water. With intact HCl and HBr, the absorption spectra of the $HX-(H_2O)_n$ clusters evolve quite closely to what has been recorded for bare water clusters. HCl and HBr have again a very similar effect on the water cluster absorption as another water molecule. The shape of the spectra also changes upon a complexation because the X−H and O−H bonds (which mostly govern the shape of the spectra) have vibrational frequencies red-shifted with respect to bare molecules. Thus we can observe an increasing width with an increasing cluster size and at the same time a blue shift of the absorption maximum for these spectra.

E. Shift of Electronic Absorption Spectra upon Acidic Dissociation. We have calculated spectra for $HX(H_2O)_4$ clusters (X = F, Cl, Br) both in a covalent state (with the intact HX molecule) and in an ionic state. We have considered two types of ionic structures: contact pairs $X^-H_3O^+(H_2O)_3$ and solvent separated pairs, in which the halogenide anion and oxonium cation are separated by solvent molecules $X^-(H_2O)_3H_3O^+$.

Hydrogen fluoride is different from the other two hydrogen halides. It is a weak acid that dissociates only to a small extent. As discussed above, we were able to localize the minimum corresponding to a solvent separated pair for $HF(H_2O)_4$; however, we were not able to find a truly contact ion minimum. On the other hand, the HF distance can be for certain structures quite elongated and delocalized. HF acts differently from the point of view of the electronic excitation process (Figure 5a).

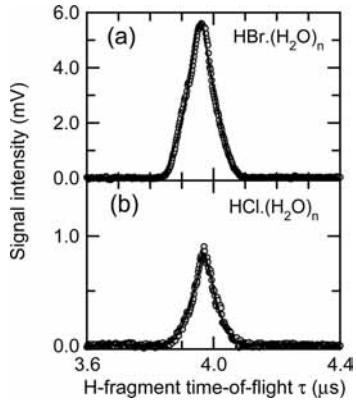

Figure 6. TOF spectra from photolysis of (a) HBr and (b) HCl on $(H_2O)_n$, $\bar{n} = 400$, clusters.

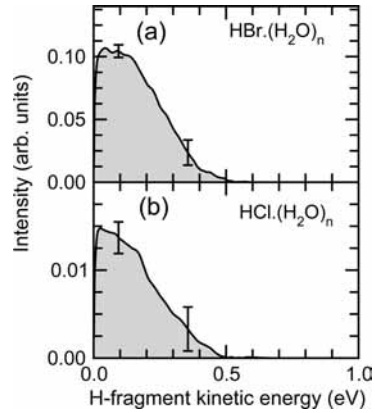

Figure 7. KED spectra from photolysis of (a) HBr and (b) HCl on $(H_2O)_n$, $\bar{n} = 400$, clusters.

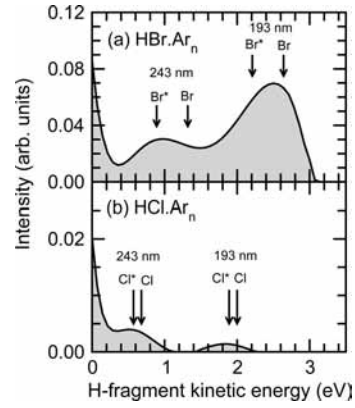

Figure 8. KED spectra from photolysis of (a) HBr and (b) HCl on Ar_n, $\bar{n} = 100$, clusters.

For the intact structure, hydrogen fluoride is just a spectator molecule, not involved in an excitation above 190 nm. This remains true even after the acidic dissociation. Low lying excited states result from an excitation within the water molecules and the fluoride anion is not directly involved. The electrostatic effect is, however, stronger for the fluoride anion than for HF. As a result, the absorption maximum shifts further to the blue.

On the other hand, the electronic absorption spectra of $HCl(H_2O)_4$ and $HBr(H_2O)_4$ clusters are significantly red-shifted with the acidic dissociation (Figure 5b,c). The position of the maximum shifts from 153 nm to approximately 180 nm for $HCl(H_2O)_4$ and to 210 nm for $HBr(H_2O)_4$. Importantly, this shift leads to the huge enhancement of the photoabsorption cross section at 193 nm for HCl. The photoabsorption cross section at 193 nm increases also for HBr but to a lesser extent than in the case of HCl. Chloride and bromide anions are directly involved in the photoexcitation process. For the intact structure, the first excited state is mostly connected with excitations within the HX molecule, after the acidic dissociation the excitation adopts the charge-transfer-to-solvent character; *i.e.*, an electron is promoted from the X^- moiety to orbitals of the water solvent. This CTTS band falls into the spectral range of our photodissociation experiment and can thus be probed.

F. Measurements of Photodissociation of Hydrogen Halides Attached to Clusters. The absorption cross section of HBr and HCl at 193 nm is approximately 2×10^{-18} and 8×10^{-20} cm^2 molecule^{-1}, respectively.[69,70] This yields the ratio of approximately 25 for photodissociation of HBr *vs* HCl at 193 nm. Therefore, the background signal from gas phase HBr was observed when the photolysis of HBr on large water clusters was measured in our experiment, whereas no background was detected from HCl under almost identical experimental conditions. On the other hand, the H-atom signals from the photolysis of HBr and HCl on water clusters in our experiments were of the same order of magnitude. This was the very first hint that the much smaller cross section for HCl *vs* HBr becomes comparable, when the molecules are deposited on water clusters.

Figure 6 shows the measured TOF spectra of H-atom fragments from photolysis of HX on $(H_2O)_n$, $\bar{n} \approx 400$, clusters. The ratio of the integrated signals from the HBr *vs* HCl photodissociation is 7.5. However, the signals should be compared after the conversion to the KED, as outlined in the experimental section. The corresponding KEDs are shown in Figure 7. The differences in shape between the two distributions are within the error bars indicating the confidence intervals for the fits used in the TOF → KED conversion. This supports the conclusion that the spectra result from the hydronium H_3O dissociation in both HBr and HCl cases, as discussed elsewhere.[37] The KED integral ratio is in an agreement with the TOF spectra ratio above. Repetitive measurements for various experimental conditions resulted in the ratio of 7.4 ± 1.0 for $HBr(H_2O)_n$ *vs* $HCl(H_2O)_n$ photolysis.

Because we argue that the lower intensity ratio from HX photolysis for HBr *vs* HCl on water clusters is a consequence of the acidic dissociation, we have also measured the photolysis of HX on Ar_n clusters, where acidic dissociation is impossible. Here, the situation is quite different. As already established in our previous detailed investigation of these systems, the photolysis of HBr on Ar_n clusters yields some fast H-fragments with energies up to ~3 eV, whereas the photolysis of HCl results in strong caging and mostly low energy fragments below 1 eV. This is illustrated by the corresponding KEDs in Figure 8. The features of the KEDs were discussed in detail in our previous publication.[50] The ratio of 20 ± 5 was obtained from these measurements for the photodissociation of HBr *vs* HCl on Ar_n clusters. A bigger error here is due to the contribution of the fast fragments. The detection probability for the fast fragments is, indeed, much smaller than for the slow ones, resulting in the larger ambiguity of the corresponding TOF spectra fits. This ratio agrees within the error bars with the gas phase absorption cross section ratio.

An additional effort has been made to prove that our procedure of the TOF → KED conversion yields correct ratios. The photodissociation of gas phase HX was measured as described in the experimental section. This results in the ratio of 23 ± 5 for the molecules quite in an agreement with the gas phase absorption cross sections.

TABLE 3: Comparison of Calculated and Experimental Ratios of the Photolysis Rate of HCl to HBr *j*(HBr)/*j*(HCl) in Different Environments and Dissociation States

measured system	measured ratio	calculated structure motif	calculated ratio
bare HX molecule	23 ± 5	bare HX molecule	≥ 30[a]
$HX(Ar_{100})$	20 ± 5		
$HX(H_2O)_{400}$	7.4 ± 1.0	$HX(H_2O)_4$ dissociated	2.7 (1.8)[b]
		$HX(H_2O)_4$ intact	≥ 45[a]

[a] These values have been obtained by extrapolation from shorter wavelengths. [b] The first number refers to the contact ion pair, number in parenthesis to the solvent separated ion.

IV. Discussion

The major findings of our calculations can be summarized as follows: (i) Addition of HF, HCl, HBr or of another water molecule to a water molecule or water cluster leads to a slight blue shift in the electronic absorption spectrum. (ii) Acidic dissociation of HCl and HBr leads to a significant red shift in the absorption spectrum; in fact, a new CTTS band appears. In the case of hydrogen fluoride, the CTTS band does not appear and F^- only acts as a counterion. We argue here that the CTTS band provides an important spectroscopically observable clue of the acidic dissociation. There are thus two major interconnected questions to be discussed: (1) Are the calculations supported by our recent photodissociation experiments? (2) Are HCl and HBr acidically dissociated under the experimental conditions?

According to our calculations, measuring the absorption cross section in the region between 180 and 250 nm should answer the question whether hydrogen halides have been in a dissociated state or not. We have measured the H-atom photodissociation yield corresponding to the absorption cross section. The photolysis rate and the absorption cross section are related by

$$j = \int_\lambda \sigma(\lambda)\, \varphi(\lambda)\, F(\lambda)\, \mathrm{d}\lambda \qquad (3)$$

where $\sigma(\lambda)$ is the absorption cross section, $\varphi(\lambda)$ is the photodissociation quantum yield and $F(\lambda)$ is the photon flux at wavelength λ. The photon fluxes from the two lasers in our experiment were sharply peaked around 193 and 243 nm and they have been approximately equal. If we assume the hydrogen atom to be the only product, *i.e.*, $\varphi(\lambda) = 1$, then the measured amount of hydrogen atoms is proportional to the absorption cross section at 193 and 243 nm. We do not obtain absolute values of the absorption cross section but relative values between different species at a given wavelength can be compared.

First, it is worthwhile to note that a measured signal increases by an order of magnitude upon the hydrogen halide deposition on a water nanoparticle. Of course, both HCl and HBr have larger absorption cross sections than water at 193 nm (absorption of all species is much smaller at 243 nm). On the other hand, there is a huge excess of water molecules, the ratio being approximately 400. Although the presence of HBr could explain the order-of-magnitude increase, this is not the case for HCl. We can, however, easily understand the observed intensity increase considering an acidically dissociated state of HCl.

The quantity for which the theoretical prediction can be directly compared with the photodissociation experiment is the ratio of hydrogen atom yields produced from HCl and HBr in different environments. These ratios are compared to the values calculated for model $HX(H_2O)_4$ clusters in Table 3. We discuss in detail below that both in the experiment and in theory this ratio significantly drops upon an acidic dissociation. As previously noted, the ratio for bare hydrogen halides (calculated from refs 69 and 70) should be about 25. Indeed, such a ratio has been recorded in our photodissociation experiment. The electronic absorption spectrum of hydrogen halides is not significantly influenced by the presence of rare gas atoms. The presence of rare gas atoms leads to the slowing down of outgoing hydrogen atoms[49,50] but the amount of hydrogen atoms produced should not change. This conclusion is again supported by our measurements, leading to the estimated *j*(HBr)/*j*(HCl) ratio of 20 ± 5. The same ratio measured for hydrogen halides deposited on the surface of water clusters leads to 7.4 ± 1. In our experiment, photons of the two wavelengths are actually present, therefore

$$\frac{j(\mathrm{HBr})}{j(\mathrm{HCl})} = \frac{(\sigma_{193}(\mathrm{HBr}) + \sigma_{243}(\mathrm{HBr}))}{(\sigma_{193}(\mathrm{HCl}) + \sigma_{243}(\mathrm{HCl}))} \qquad (4)$$

which yields a theoretically predicted ratio of the photolysis of about 2.7 for the contact ion and 1.8 for the solvent separated ion structure (see Table 3). A theoretical estimate of this ratio for the intact structure (as well as for bare HX from our calculations) is difficult because even at the 193 nm we sample only the very red tail of the HCl spectrum. Nevertheless, by an extrapolation one can conclude that the ratio exceeds 30 for a bare molecule. (Higher values of *j*(HBr)/*j*(HCl) factor with respect to the experiment are given by the harmonic approximation engaged.) We even observe a further increase of this factor upon the complexation with water. Therefore, the comparison strongly suggests that the acidic dissociation takes place. It should be noted that the qualitative change between argon and water clusters could not be otherwise explained.

The measured ratio still somewhat exceeds the theoretical prediction of the *j*(HBr)/*j*(HCl) ratio, which leaves open a possibility that a certain fraction of hydrogen halides could stay intact. It is, however, more likely that the precise quantitative agreement is not achieved due to the comparison of theoretical calculations performed for small water clusters with experiment on much larger clusters. Also, the TDDFT calculations may introduce some error. Furthermore note that the σ(HBr)/σ(HCl) ratio is a steep function of wavelength around 193 nm (for a contact ion irradiated with 200 nm the theoretical ratio *j*(HBr)/*j*(HCl) would be 4.4, for solvent separated ion 2.2). The precise numerical value of the calculated *j*(HBr)/*j*(HCl) ratio can change to certain extent upon an inclusion of the highly anharmonic low frequency modes into the ground state sampling. The conclusion that the *j*(HBr)/*j*(HCl) ratio drops upon an acidic dissociation is, however, robust.

As we have mentioned in the Introduction, one particularly important photochemical system is the atmosphere of the Earth. It is interesting to explore how the acidic dissociation influences the photolysis rate of hydrogen halides. Here again, we limit our attention to HCl and HBr because of their atmospheric significance. The photolysis rate is given by eq 3. The actinic flux $F(\lambda)$ is an increasing function of the altitude. In the stratosphere, the actinic flux drops at about 300 nm and then somewhat increases around 200 nm. The intensity again drops below 180 nm.[71] The acidic dissociation shifts the electronic absorption spectrum to the red, so that it can be expected that the photolysis rate will be much enhanced when hydrogen halide lands on a water cluster. To quantify this issue, we have supplied eq 3 with the actinic flux measured at the altitude of 50 km. The photolysis rate has increased by 4 orders of magnitude upon the HCl uptake and dissociation on $(H_2O)_4$ cluster, the enhancement for HBr was 2 orders of magnitude. We estimate that the photolysis rate of $H^+(H_2O)_4Cl^-$ is about $^1/_{20}$th to $^1/_{10}$th

of the photolysis of molecular chlorine (Cl_2). Ice nanoparticles thus might catalyze the HCl photolysis in a way that can potentially play a non-negligible role in the stratospheric chlorine budget.

Although the major interest in this paper are water clusters doped with hydrogen halides, we have also explored absorption cross sections of bare water clusters. These calculations are, to the best of our knowledge, the first *ab initio* calculations addressing the question of the shape of the absorption spectrum for water clusters. Note that our calculated spectra connect the electronic absorption spectra of isolated water molecules with the ones measured for a condensed phase. Previous calculations based on a model water potential[38] have predicted large blue shifts in water upon a complexation. For a water dimer, on the other hand, a red tail has been predicted. In our *ab initio* electronic absorption spectra calculations we were still able to see a red tail for a water dimer and generally a blue shift with increasing size of water clusters, in agreement with another theoretical study.[41] However, our calculated blue shift is significantly smaller than the one presented by Harvey *et al*.[38]

During the discussion, we have singled out hydrogen fluoride. The reason is 2-fold: the hydrogen fluoride−water system has not been measured. Also, hydrogen fluoride differs from HCl and HBr both in the ground and in the excited states: It is a weak acid and it absorbs at shorter wavelengths. Note that even for HF measuring the electronic absorption spectra or quantities related to the absorption cross section can bring information on a state of this system in the ground state. The water absorption spectrum is shifted to the blue upon the HF attachment and there is a more significant shift upon the acidic dissociation.

V. Conclusions

By a joint theoretical and experimental effort we have shown that for temperatures near 120 K extensive acidic dissociation of HCl and HBr is observed on ice nanoparticles and photoactive products are formed. Theoretically, we have modeled absorption spectra of $HF(H_2O)_N$, $HCl(H_2O)_N$, $HBr(H_2O)_N$ and $(H_2O)_N$ molecular clusters for $N = 0-5$ using the reflection principle. Three structural types have been considered: clusters with intact HX, contact ion structures and solvent separated ion pairs. The major findings can be summarized as follows: (i) The electronic absorption spectrum of water clusters shifts to shorter wavelengths with an increasing cluster size, rapidly converging to the absorption spectrum of bulk water. (ii) The first absorption band of $HF(H_2O)_N$ clusters is dominated by water absorption regardless of a ground state structure. (iii) For $HCl(H_2O)_N$ and $HBr(H_2O)_N$ clusters, the absorption maxima shift toward lower wavelengths for intact structures with increasing N. However, upon either partial or full acidic dissociation of HX the charge-transfer-to-solvent band emerges. This CTTS band shifts the onset of the absorption spectrum by 40−60 nm to larger wavelengths for both HCl and HBr.

Experimentally, we have measured the relative H-atom yield in the photodissociation experiments for HBr *vs* HCl molecules attached to $(H_2O)_N$ clusters, $\bar{N} = 400$. Our calculations were quantitatively compared with this photodissociation experiment. We conclude that for ice nanoparticles of an average temperature 100−130 K heavier hydrogen halides (HCl and HBr) acidically dissociate on the cluster surface. Upon the electronic excitation into the CTTS band, the H_3O radical and halogen atom are formed. Hydrogen halide molecules become much more susceptible to the atmospheric photodissociation upon the acidic dissociation. This may possibly play a role in the modeling of the reactive halogen species in the atmosphere.

Acknowledgment. Support by the special program "Nanotechnology for society" of the Czech Academy of Sciences *via* grant No. KAN400400651 and grant No. 203/06/1290 of the Grant Agency of the Czech Republic. P.S. also acknowledges postdoctoral grant No. 203/07/P449 and computational support of the research center LC512 and M.F. acknowledges a special J. E. Purkyně fellowship of the Czech Academy of Sciences.

Supporting Information Available: Cartesian coordinates of the clusters depicted in Figure 2; full citations for refs 54 and 55. This material is available free of charge *via* the Internet at http://pubs.acs.org.

References and Notes

(1) Finlayson-Pitts, B. J.; Pitts, J. N., Jr. *Chemistry of the Upper and Lower Atmosphere*; Academic Press: San Diego, 2000.
(2) Peter, T. *Annu. Rev. Phys. Chem.* **1997**, *48*, 785.
(3) Molina, M. J.; Tso, T. L.; Molina, L. T.; Wang, F. C. Y. *Science* **1987**, *238*, 1253.
(4) Huthwelker, T.; Ammann, M.; Peter, T. *Chem. Rev.* **2006**, *106*, 1375.
(5) McNeill, V. F.; Geiger, F. M.; Loerting, T.; Trout, B. L.; Molina, L. T.; Molina, M. J. *J. Phys. Chem. A* **2007**, *111*, 6274.
(6) Buch, V.; Sadlej, J.; Aytemiz-Uras, N.; Devlin, J. P. *J. Phys. Chem. A* **2002**, *106*, 9374.
(7) Devlin, J. P.; Uras, N.; Sadlej, J.; Buch, V. *Nature* **2002**, *417*, 269.
(8) Devlin, J. P.; Fárník, M.; Suhm, M. A.; Buch, V. *J. Phys. Chem. A* **2005**, *109*, 955.
(9) Voegele, A. F.; Liedl, K. R. *Angew. Chem., Int. Ed.* **2003**, *42*, 2114.
(10) Hurley, S. M.; Dermota, T. E.; Hydutsky, D. P.; Castleman, A. W. *Science* **2002**, *298*, 202.
(11) Ayotte, P.; Hebert, M.; Marchand, P. *J. Chem. Phys.* **2005**, *123*, 184501.
(12) Kang, H.; Shin, T. H.; Park, S. C.; Kim, I. K.; Han, S. J. *J. Am. Chem. Soc.* **2000**, *122*, 9842.
(13) Park, S. C.; Kang, H. *J. Phys. Chem. B* **2005**, *109*, 5124.
(14) Parent, P.; Laffon, C. *J. Phys. Chem. B* **2005**, *109*, 1547.
(15) Kondo, M.; Kawanowa, H.; Gotoh, Y.; Souda, R. *J. Chem. Phys.* **2004**, *121*, 8589.
(16) Yabushita, A.; Kanda, D.; Kawanaka, N.; Kawasaki, M. *J. Chem. Phys.* **2007**, *127*, 154721.
(17) Al-Halabi, A.; Bianco, R.; Hynes, J. T. *J. Phys. Chem. A* **2002**, *106*, 7639.
(18) Re, S.; Osamura, Y.; Suzuki, Y.; Schaefer, H. F. *J. Chem. Phys.* **1998**, *109*, 973.
(19) Conley, C.; Tao, F. M. *Chem. Phys. Lett.* **1999**, *301*, 29.
(20) Cabaleiro-Lago, E. M.; Hermida-Ramon, J. M.; Rodriguez-Otero, J. *J. Chem. Phys.* **2002**, *117*, 3160.
(21) Weimann, M.; Fárník, M.; Suhm, M. A. *Phys. Chem. Chem. Phys.* **2002**, *4*, 3933.
(22) Fárník, M.; Weimann, M.; Suhm, M. A. *J. Chem. Phys.* **2003**, *118*, 10120.
(23) Kuo, J. L.; Klein, M. L. *J. Chem. Phys.* **2004**, *120*, 4690.
(24) Odde, S.; Mhin, B. J.; Lee, S.; Lee, H. M.; Kim, K. S. *J. Chem. Phys.* **2004**, *120*, 9524.
(25) Goursot, A.; Fischer, G.; Lovallo, C. C.; Salahub, D. R. *Theor. Chem. Acc.* **2005**, *114*, 115.
(26) Masia, M.; Forbert, H.; Marx, D. *J. Phys. Chem. A* **2007**, *111*, 12181.
(27) Ndongmouo, U. F. T.; Lee, M. S.; Rousseau, R.; Baletto, F.; Scandolo, S. *J. Phys. Chem. A* **2007**, *111*, 12810.
(28) Buch, V.; Bauerecker, S.; Devlin, J. P.; Buck, U.; Kazimirski, J. K. *Int. Rev. Phys. Chem.* **2004**, *23*, 375.
(29) Slavíček, P.; Jungwirth, P.; Lewerenz, M.; Nahler, N. H.; Fárník, M.; Buck, U. *J. Phys. Chem. A* **2003**, *107*, 7743.
(30) Woittequand, S.; Toubin, C.; Pouilly, B.; Monnerville, M.; Briquez, S.; Meyer, H. D. *Chem. Phys. Lett.* **2005**, *406*, 202.
(31) Woittequand, S.; Duflot, D.; Monnerville, M.; Pouilly, B.; Toubin, C.; Briquez, S.; Meyer, H. D. *J. Chem. Phys.* **2007**, *127*, 164717.
(32) Hurley, S. M.; Dermota, T. E.; Hydutsky, D. P.; Castleman, A. W. *J. Chem. Phys.* **2003**, *118*, 9272.
(33) Dermota, T. E.; Hydutsky, D. P.; Bianco, N. J.; Castleman, A. W. *J. Chem. Phys.* **2005**, *123*, 214308.
(34) Sobolewski, A. L.; Domcke, W. *J. Phys. Chem. A* **2003**, *107*, 1557.
(35) Sobolewski, A. L.; Domcke, W. *Phys. Chem. Chem. Phys.* **2005**, *7*, 970.
(36) Sobolewski, A. L.; Domcke, W. *J. Phys. Chem. A* **2007**, *111*, 11725.
(37) Poterya, V.; Fárník, M.; Slavíček, P.; Buck, U.; Kresin, V. V. *J. Chem. Phys.* **2007**, *126*, 071101.

(38) Harvey, J. N.; Jung, J. O.; Gerber, R. B. *J. Chem. Phys.* **1998**, *109*, 8747.
(39) Bursulaya, B. D.; Jeon, J.; Yang, C. N.; Kim, H. J. *J. Phys. Chem. A* **2000**, *104*, 45.
(40) Miller, Y.; Fredj, E.; Harvey, J. N.; Gerber, R. B. *J. Phys. Chem. A* **2004**, *108*, 4405.
(41) Chipman, D. M. *J. Chem. Phys.* **2005**, *122*, 044111.
(42) Sobolewski, A. L.; Domcke, W. *J. Chem. Phys.* **2005**, *122*, 184320.
(43) Garbuio, V.; Cascella, M.; Reining, L.; Del Sole, R.; Pulci, O. *Phys. Rev. Lett.* **2006**, *97*, 137402.
(44) do Couto, P. C.; Cabral, B. J. C. *J. Chem. Phys.* **2007**, *126*, 014509.
(45) Yabushita, A.; Hashikawa, Y.; Ikeda, A.; Kawasaki, M.; Tachikawa, H. *J. Chem. Phys.* **2004**, *120*, 5463.
(46) Andersson, S.; Kroes, G. J.; van Dishoeck, E. F. *Chem. Phys. Lett.* **2005**, *408*, 415.
(47) Andersson, S.; Al-Halabi, A.; Kroes, G. J.; van Dishoeck, E. F. *J. Chem. Phys.* **2006**, *124*, 064715.
(48) Yabushita, A.; Kanda, D.; Kawanaka, N.; Kawasaki, M.; Ashfold, M. N. R. *J. Chem. Phys.* **2006**, *125*, 133406.
(49) Slavíček, P.; Jungwirth, P.; Lewerenz, M.; Nahler, N. H.; Fárník, M.; Buck, U. *J. Chem. Phys.* **2004**, *120*, 4498.
(50) Fárník, M.; Nahler, N. H.; Buck, U.; Slavíček, P.; Jungwirth, P. *Chem. Phys.* **2005**, *315*, 161.
(51) Bergner, A.; Dolg, M.; Kuchle, W.; Stoll, H.; Preuss, H. *Mol. Phys.* **1993**, *80*, 1431.
(52) Magyar, R. J.; Tretiak, S. *J. Chem. Theory Comput.* **2007**, *3*, 976.
(53) Zhao, Y.; Gonzalez-Garcia, N.; Truhlar, D. G. *J. Phys. Chem. A* **2005**, *109*, 2012.
(54) Werner, H.-J. et.al,MOLPRO, version 2006.1, a package of *ab initio* programs, 2006., see http://www.molpro.net.
(55) Frisch, M. J.; et. al. *Gaussian 03*, revision 0.02; Gaussian, Inc.: Wallingford, CT, 2004.
(56) Prakash, M. K.; Weibel, J. D.; Marcus, R. A. *J. Geophys. Res.* **2005**, *110*, D21315.
(57) Grage, M. M. L.; Nyman, G.; Johnson, M. S. *Phys. Chem. Chem. Phys.* **2006**, *8*, 4798.
(58) Della Sala, F.; Rousseau, R.; Gorling, A.; Marx, D. *Phys. Rev. Lett.* **2004**, *92*, 183401.
(59) Buck, U. *J. Phys. Chem. A* **2002**, *106*, 10049.
(60) Bobbert, C.; Schütte, S.; Steinbach, C.; Buck, U. *Europ. Phys. J. D* **2002**, *19*, 183.
(61) Brudermann, J.; Buck, U.; Buch, V. *J. Phys. Chem. A* **2002**, *106*, 453.
(62) Baumfalk, R.; Buck, U.; Frischkorn, C.; Nahler, N. H.; Hüwel, L. *J. Chem. Phys.* **1999**, *111*, 2595.
(63) Liu, K.; Brown, M. G.; Carter, C.; Saykally, R. J.; Gregory, J. K.; Clary, D. C. *Nature* **1996**, *381*, 501.
(64) Slavíček, P.; Roeselová, M.; Jungwirth, P.; Schmidt, B. *J. Chem. Phys.* **2001**, *114*, 1539.
(65) Kawasaki, M.; Sugita, A.; Ramos, C.; Matsumi, Y.; Tachikawa, H. *J. Phys. Chem. A* **2004**, *108*, 8119.
(66) Mota, R.; Parafita, R.; Giuliani, A.; Hubin-Franskin, M. J.; Lourenço, J. M. C.; Garcia, G.; Hoffmann, S. V.; Mason, N. J.; Ribeiro, P. A.; Raposo, M.; Limao-Vieira, P. *Chem. Phys. Lett.* **2005**, *416*, 152.
(67) Heller, J. M.; Hamm, R. N.; Birkhoff, R. D.; Painter, L. R. *J. Chem. Phys.* **1974**, *60*, 3483.
(68) Kobayashi, K. *J. Phys. Chem.* **1983**, *87*, 4317.
(69) Nee, J. B.; Suto, M.; Lee, L. C. *J. Chem. Phys.* **1986**, *85*, 4919.
(70) Cheng, B. M.; Chung, C. Y.; Bahou, M.; Lee, Y. P.; Lee, L. C. *J. Chem. Phys.* **2002**, *117*, 4293.
(71) DeMore, W. B.; Sander, S. P.; Golden, D. M.; Hampson, R. F.; Kurylo, M. J.; Howard, C. J.; Ravishankara, A. R.; Kolb, C. E.; Molina, M. J. *Chemical Kinetics and Photochemical Data for Use in Stratospheric Modeling*; JPL Publication 97-4; Jet Propulsion Laboratory: Pasadena, CA, 1997.

JP8012305